Inorganic Chemistry

Article

pubs.acs.org/IC

# Gold(I) Complexes of Brominated Azadipyrromethene Ligands

Lei Gao, Nihal Deligonul, and Thomas G. Gray*

Department of Chemistry, Case Western Reserve University, 10900 Euclid Avenue, Cleveland Ohio 44106, United States

Supporting Information

**ABSTRACT:** Azadipyrromethenes are luminescent, red-light absorbing dyes that readily bind $BF_2^+$ and metals. Their framework allows for structural modification at the phenyl arms and the two pyrrolic carbon positions. Here we report five new gold(I) complexes with azadipyrromethene ligands brominated at the pyrrolic carbons and/or the four phenyl substituents. New complexes are characterized by multinuclear NMR spectroscopy, X-ray crystallography, optical absorption and emission spectroscopy, and elemental analysis. The new compounds have a perturbed two-coordinate geometry in the crystalline state, with gold(I) binding one dimethylphenylphosphine ancillary ligand and one pyrrole nitrogen of the azadipyrromethene. The second azadipyrromethene pyrrole nitrogen perturbs the linear coordination. These complexes maintain the absorption features of the free ligands. Excitation in the near-ultraviolet generates emission in the near-UV and visible regions. Density-functional theory calculations indicate that the photoproperties of the new compounds arise almost entirely from the conjugated ligands and not from the (phosphine)gold(I) fragments.

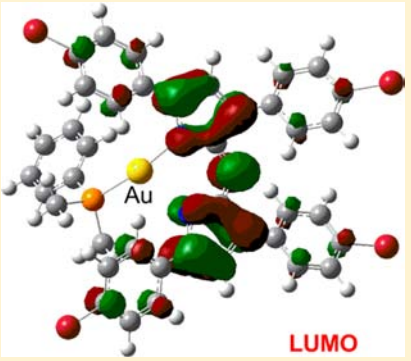


## INTRODUCTION

Azadipyrromethenes are nitrogenous pigments that bind $BF_2^+$ and chelate metal ions. In recent years, they have emerged as photodynamic therapy mediators, luminescent probes, and light harvesters.[1−3] Most azadipyrromethenes are synthesized from chalcone precursors that themselves derive from reactions of aldehydes with acetophenones. Thus, the typical azadipyrromethene has four aryl substituents, denoted proximal and distal below. The proximal aryls derive from an acetophenone; the distal aryls, from an aldehyde. The aryl arms can carry substituents, and aryl modification is a ready way of modulating the optical properties of azadipyrromethene complexes. Substitution also occurs at the pyrrolic carbon with suitable electrophiles. If the distal arms carry Lewis basic sites, then azadipyrromethenes potentially become tridentate ligands.[4] If the proximal arms do so, then tetradentate ligands result.[5]

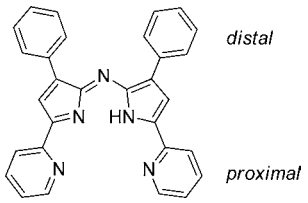


The coordination chemistry of azadipyrromethene ligands is steadily emerging. Bidentate azadipyrromethene complexes have been characterized for zinc and mercury,[6] rhenium(I),[7] the coinage metals,[8,9] and nickel(II), cobalt(II), and iron(II).[10] When bound to metals, azadipyrromethenes retain their chromophoric character. INDO/S[6] and density-functional theory calculations[8,9] find that the frontier orbitals, at least of $d^{10}$-complexes, reside on the ligand $\pi$-system. As with porphyrins,[11] configuration interaction is prominent for azadipyrromethene ligands. An intense visible absorption near 600 nm results from a linear combination of one-electron transitions involving the lowest unoccupied molecular orbital (LUMO), highest occupied molecular orbital (HOMO), and HOMO − 1. In zinc bis(azadipyrromethene) complexes, visible light absorption is broader. As many as four transitions are involved.[6]

Boron azadipyrromethenes are visible (red) fluorophores, even when substituted with heavy atoms such as bromine. An ongoing need is to design emitters of near-infrared light for use in solar cells and light-emitting diodes, and as heat-absorbers and bioimaging dyes.[12,13] Results from this laboratory[14−21] and elsewhere[22−24] show that binding even a single gold atom to organic fluorophores generates phosphorescence while quenching fluorescence. Our earlier study[8] of a gold(I) complex of an unsubstituted tetraarylazadipyrromethene found only fluorescence, with a small Stokes shift and no evidence of triplet emission. Here we report a series of (phosphine)gold(I) complexes of brominated azadipyrromethene ligands. Three new complexes are characterized crystallographically. Several show dual emission with the usual azadipyrromethene fluorescence and a new, broad emission at longer wavelengths.

## RESULTS AND DISCUSSION

**Syntheses.** Scheme 1 enumerates azadipyrromethene ligands and complexes, and summarizes their syntheses. The free ligands were prepared by the methods of O'Shea and coworkers.[1] Ligands $\mathbf{L}_{a-c}$ are known; $\mathbf{L}_d$ is new. Bromination at the pyrrolic carbon atoms ($\mathbf{L}_{a-d}\mathbf{Br}_2$ series) was effected with *N*-bromosuccinimide (NBS).[25] The isolated azadipyrromethene

**Received:** April 5, 2012
**Published:** July 3, 2012

   dx.doi.org/10.1021/ic300709n | *Inorg. Chem.* 2012, 51, 7682−7688

**Scheme 1**

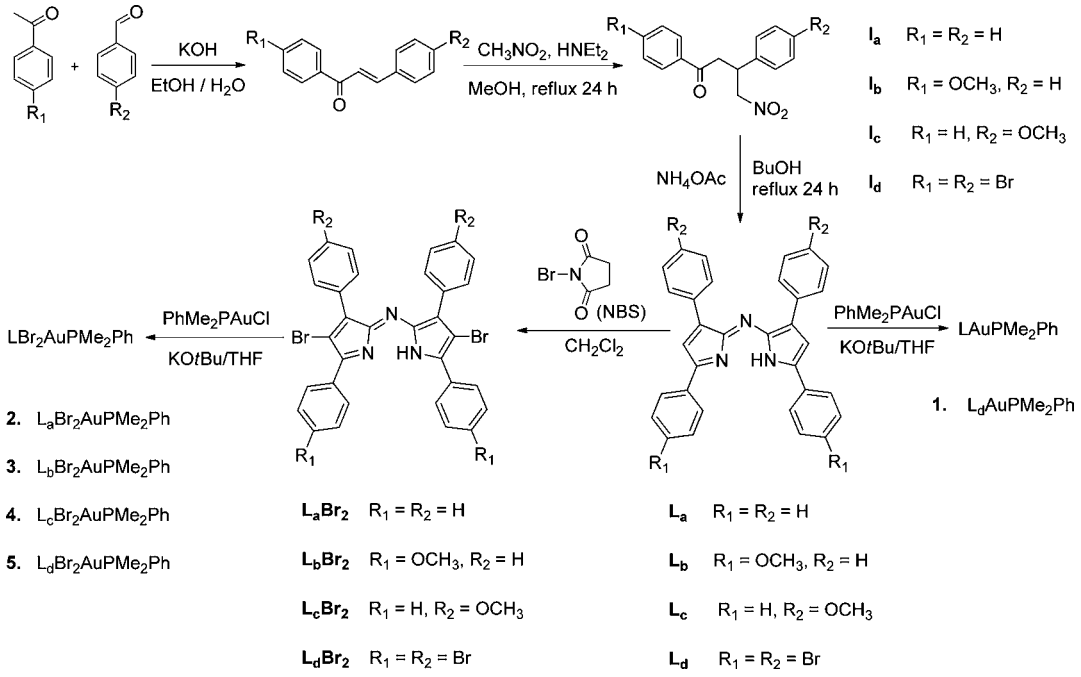


complexes were stirred with 2 equiv of *N*-bromosuccinimide (NBS) in dichloromethane. Dark precipitates of $\mathbf{L_{a-d}Br_2}$ formed quickly. The products were purified by washing with dichloromethane. They are sparingly soluble in organic solvents and can be used in the synthesis of gold(I) complexes without further purification.

The free ligands were deprotonated with 2 equiv of KO*t*Bu or NaO*t*Bu in tetrahydrofuran (THF). The ligands solubilize upon adding base, and a homogeneous turquoise solution results. The reaction mixture was deoxygenated and stirred under argon for a period of hours. The gold(I) starting material, $Me_2PhPAuCl$, was added to the reaction flask under air. The use of $PMe_2Ph$ as ancillary ligand is motivated by its smaller size compared to $PPh_3$ ($\Theta$ = 122° vs 145°, respectively)[26] which we have employed on earlier work[8] on group 11 azadipyrromethene complexes. The solution was again purged with argon, and the resulting turquoise-colored mixture was stirred for 48 h. The solvent was stripped under vacuum to leave a lustrous red solid. This residue was redissolved in benzene, and the benzene solution was filtered through Celite. The filtrate was evaporated to dryness. Triturating the residue with pentane led to the isolation of gold(I) azadipyrromethene complexes as iridescent red powders. Analytically pure materials resulted from vapor diffusion of *n*-pentane into benzene solutions or layering *n*-pentane onto benzene solutions. Crystals of compounds **1**, **2**, and **4** take on a lustrous red color, and **3** has a green tint. A greenish powder was collected for **5** after crystallization.

$^{31}P\{^1H\}$ NMR confirms the binding of gold to the azadipyrromethene ligand. The $^{31}P\{^1H\}$ resonance of free $PMe_2Ph$ occurs at −46.0 ppm, and that of $Me_2PhPAuCl$ appears at 4.2 ppm. Coordination of the AuCl group induces a 50-ppm downfield shift. Collected in Table S1, Supporting Information, are $^{31}P\{^1H\}$ chemical shifts of the new gold(I) complexes. Compared with $Me_2PhPAuCl$, an upfield shift of 5−6 ppm occurs in the new complexes. Successive bromination of the azadipyrromethene ligand shifts the $^{31}P\{^1H\}$ resonance upfield; resonances for **1** and **5** are further upfield than those of **2**−**4**. The electronic effect of the methoxy substituents is less, based on $^{31}P\{^1H\}$ NMR. Compounds **2**, **3**, and **4** have similar $^{31}P\{^1H\}$ chemical shifts. Upon binding to the $Me_2PhPAu^+$ fragment, a 0.1−0.4 ppm downfield shift of the *meta* and *ortho* protons of the proximal azadipyrromethene phenyl substituents occurs. The doublet assigned to the methyl groups on $PMe_2Ph$ shifts upfield by 0.1−0.3 ppm.

**Crystallography.** Compounds **1**, **2**, and **4** have been characterized crystallographically. No aurophilic contacts are present. In all structures gold binds the azadipyrromethene ligand asymmetrically. In no case does gold have a regular, three-coordinate geometry. Coordination geometries are nearer two-coordinate, although P−Au−N angles deviate from strict linearity. Thermal ellipsoid projections of **1**, **2**, and **4** appear in Figures 1−3, respectively. Table S2, Supporting Information, assembles crystallographic data for the new complexes.

The interatomic distances of Table 1 show asymmetric gold−nitrogen binding. Atom numbers are assigned so that N1

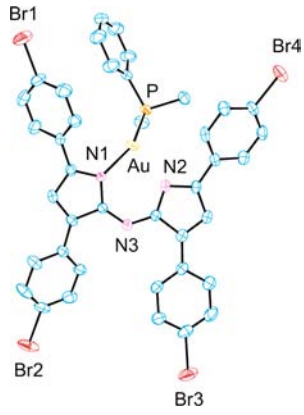


**Figure 1.** Thermal ellipsoid depiction of **1** (50% probability). Unlabeled atoms are carbon; hydrogen atoms are omitted for clarity.


dx.doi.org/10.1021/ic300709n | *Inorg. Chem.* 2012, 51, 7682−7688


**Figure 2.** Thermal ellipsoid depiction of **2** (50% probability). Unlabeled atoms are carbon; hydrogen atoms are omitted for clarity.

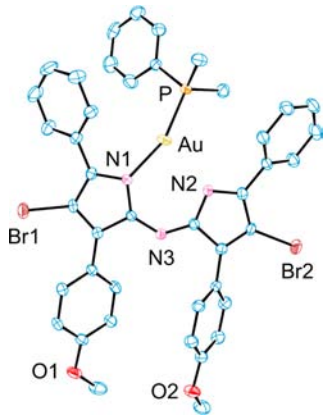


**Figure 3.** Thermal ellipsoid depiction of **4** (50% probability). Unlabeled atoms are carbon; hydrogen atoms are omitted for clarity.

**Table 1. Selected Interatomic Distances (Å) and Angles (deg) in Crystal Structures of 1, 2, and 4**

| | 1 | 2 | 4 |
|---|---|---|---|
| Au–N1 | 2.140(3) | 2.119(2) | 2.113(2) |
| Au–N2 | 2.420(4) | 2.490(2) | 2.560(2) |
| Au–P | 2.2093(12) | 2.2071(8) | 2.2179(8) |
| ∠N1–**Au**–P[a] | 155.05(9) | 158.48(7) | 160.00(7) |
| ∠P–**Au**–N2[a] | 125.29(9) | 121.57(6) | 117.44(6) |
| ∠N1–**Au**–N2[a] | 77.3 (1) | 79.78(8) | 82.44(8) |

[a]The atom in boldface type lies at the vertex of the angle.

is the nitrogen atom nearest gold and N2 is the more distant. The backbone nitrogen N3 does not bind gold. Values of the Au–N1 bond length are not significantly different over the three complexes.[27] The backbone C–$N_{meso}$–C angles are distended from an ideal 120° for $sp^2$-hybridized nitrogen. The angles range from 125.8(4)° (**1**) to 117.44(6)° (**4**). This bending back of the azadipyrromethene spine is a result of auration. The backside C–$N_{meso}$–C angle of $\mathbf{L_aBr_2}BF_2$, a typical boron chelate, is 119.5(2)°.[1]

The ligand bite angle is defined as ∠N1–Au–N2; these appear in Table 1. The bite angles of Table 1 reflect the lopsided coordination of gold(I). In **1**, **2**, and **4**, the geometry about gold accords with its tendency toward linear two-coordination.[28−32] A short bond forms to one nitrogen, and the second disturbs the N1–Au–P moiety so that it is nonlinear. The mean ∠N1–Au–P is near 158°. This arrangement is similar to that in (2,2′-bipyridine)$AuPPh_3^+$, where gold–nitrogen bond lengths are 2.166 and 2.406 Å.[33] Gold(I) in this cation might be described as perturbed, linear two-coordinate. The geometries about gold in **1**, **2**, and **4** are unlike those in our earlier gold(I) azadipyrromethene[8] or in the aminotroponiminate complexes of Roesky and co-workers.[34] In both sets of compounds, gold(I) is clearly three-coordinate, and binding is approximately trigonal.

**Optical Spectroscopy.** The absorption spectra of gold(I) azadipyrromethenes share the essential features of the free ligands. Figure 4 shows the absorption and emission spectra of

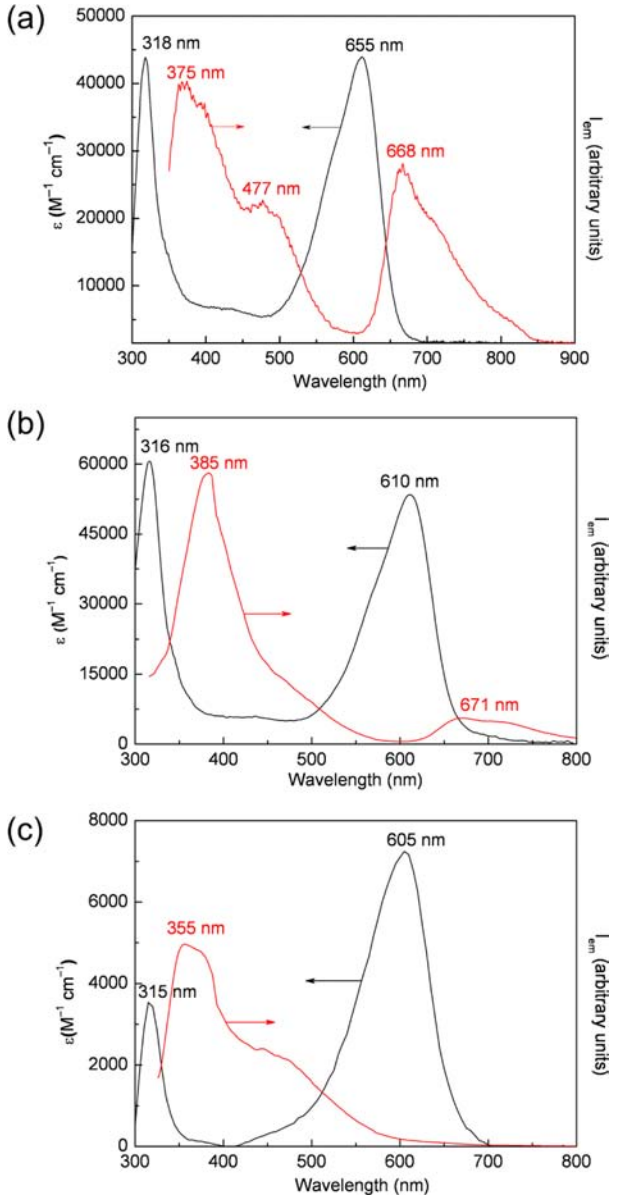


**Figure 4.** Absorption (black) and emission spectra (red) for (a) $\mathbf{L_d}$, (b) compound **1**, and (c) compound **5** in 2-MeTHF at room temperature.

$\mathbf{L_d}$, compound **1** and compound **5**; Table 2 collects absorption and emission maxima in 2-methyltetrahydrofuran (2-MeTHF). The higher-energy absorption band is largely unshifted upon metalation. The lower energy absorption peaks are sensitive to aryl substituents. The methoxy or bromo groups on the proximal phenyl arms red-shift the lower-energy peak. Methoxy substituents also cause a red shift of the higher-energy emission


dx.doi.org/10.1021/ic300709n | Inorg. Chem. 2012, 51, 7682−7688

**Table 2. Absorption and Emission Maxima of Gold(I) Azadipyrromethene Complexes and Ligands $L_{a-d}$ Recorded at Room-Temperature in 2-MeTHF**

| compound | absorption maxima (nm) | emission maxima (nm)[a] |
|---|---|---|
| $L_a$ | 308, 595 | 362, 652 |
| $L_b$ | 320, 619 | 359, 667 |
| $L_c$ | 308, 606 | 369, 672 |
| $L_d$ | 318, 655 | 375, 477, 668 |
| **1** | 316, 610 | 385, 671 |
| **2** | 309, 585 | 359 |
| **3** | 315, 400, 610 | 372, 435−500 (sh), 670 |
| **4** | 312, 595 | 372 |
| **5** | 315, 605 | 355, 435−500 (sh) |

peak. When comparing **1** with **5**, it is seen that brominating the pyrrolic positions scarcely affects the absorption profile, but the higher-energy emission peak undergoes a 30-nm blue shift.

The free ligand $L_d$ shows one emission peak at 373 nm and another broad peak around 770 nm. Both emissions are weak. Gold complexes **1**−**5** show similar emission spectra, except that two compounds emit weakly in the red. The near-ultraviolet emission of **1** is red-shifted from its value in the free ligand; it appears from 355−385 nm for **1**−**5** and strongly intensifies. The lower energy emission band appears around 700 nm with very low intensity. Emission near 700 nm, when it occurs, is feeble. It is not observable for compounds **2**, **4**, or **5**. Compound **3** shows a new absorption at 400 nm. An emission shoulder in compounds **3** and **5** appears around 435−500 nm. Optical spectra of **2**−**4** appear as Figures S1−S3, Supporting Information.

**Calculations.** Density-functional theory calculations were performed on compounds **1**−**5**. All calculations were spin-restricted. Geometries were optimized without restraint or imposed symmetry; converged metrics are acceptably near crystallographic values. Optimized structures reproduce the asymmetric chelation seen crystallographically, with rough linearity at gold. Intraligand metrics for the phosphine and the azadipyrromethenes are unexceptional.

The visible-light absorption of azadipyrromethene complexes results from an isolated, empty low-lying orbital. Figure 5 depicts a partial Kohn−Sham orbital energy level diagram of **1**, which is representative; diagrams for **2**−**5** appear as Figures S4−S7, Supporting Information. At right in Figure 5 are plots of the highest-occupied and lowest-unoccupied Kohn−Sham orbitals (HOMO and LUMO, respectively). Also shown are fractional contributions from fragment orbitals calculated according to Mulliken.[35] The HOMO and LUMO reside almost wholly on the azadipyrromethene ligand. The sizable energy gaps between HOMO and LUMO and LUMO and LUMO + 1 are consistent with the compounds' absorption profiles and with the reductive electrochemistry of azadipyrromethenes.[7] The pendant bromines of $L_d$ make small, but not insignificant, contributions to the frontier orbitals of **1**. They modulate the orbital energies and, indirectly, the energies of excited electronic states.

A time-dependent density functional theory (DFT) calculation on **1** was performed on the ground-state (singlet) geometry. The calculation included a continuum treatment of THF solvation. The computation predicts that the first singlet excited state derives from a LUMO←HOMO transition, and the vertical excitation energy is calculated to be 2.12 eV (585 nm). The corresponding LUMO←HOMO triplet is the lowest-lying triplet-state. The configuration interaction that occurs in the first excited states of Cu(I), Ag(I), and $BF_2^+$ complexes[9] is muted in **1**.

## ■ CONCLUSIONS

Brominated azadipyrromethene ligands have been prepared with *N*-bromosuccinimide as the brominating agent, or from pre-brominated aldehyde and acetophenone precursors. Among these is a ligand, $L_d$, brominated in four places, in both proximal and distal arms. These azadipyrromethene ligands bind gold in rapid reactions of $PhMe_2PAuCl$ with base in THF. Five such gold complexes were prepared; three are crystallographically characterized. The structures show that gold binds asymmetrically to these potentially chelating ligands. Coordination geometries at gold can be described as perturbed two-

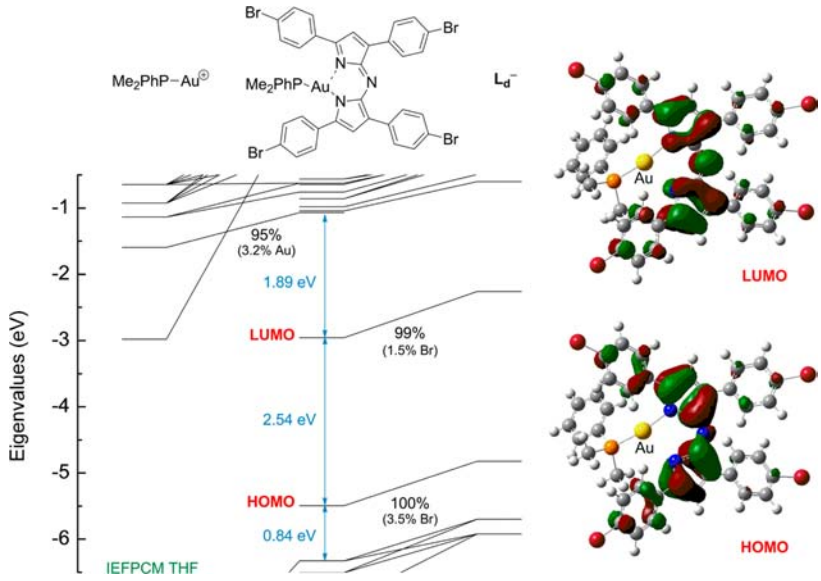


**Figure 5.** Kohn−Sham orbital energy level diagram of **1**. Percentages are of electron density. Plots of selected orbitals appear at right (contour level 0.03 au).


dx.doi.org/10.1021/ic300709n | *Inorg. Chem.* 2012, 51, 7682−7688

coordinate. The new complexes show gold(I)'s propensity to adopt a linear two-coordinate geometry, whereas gold(I) in our earlier azadipyrromethene complex is three-coordinate.

Gold(I) azadipyrromethenes reprise the absorption features of the free ligands. Excitation in the near-ultraviolet generates dual fluorescence in the near-UV and visible wavelengths. Two compounds show weak red emission that may be phosphorescence. Such an assignment is consistent with Castellano's work, which shows phosphorescence from BODIPY dyes brought about by an intramolecular triplet−triplet energy transfer from a tethered, cyclometalated iridium(III).[36]

Density-functional theory calculations indicate that the photoproperties of the new compounds arise from the azadipyrromethene ligands. Gold(I) is a perturbation. Both the HOMO and LUMO rest on the conjugated ligand, and transitions between these orbitals account for the first singlet and triplet excited states.

The bromine-substituted ligands herein commend azadipyrromethenes for incorporation into polymeric materials, such as the light-harvesting components of solar cells. Azadipyrromethenes easily bind gold(I) and baser coinage metals, and their colors and emission spectra are preserved. This ligand class also binds the *fac*-$[Re(CO)_3]^+$ fragment and 3d transition metals. Metalla-azadipyrromethenes have many exciting prospects.

## EXPERIMENTAL SECTION

**Materials.** Solvents and reagents were purchased from commercial suppliers and used without further purification unless indicated. $Me_2PhPAuCl$ and $Me_2PhPAuBr$ were synthesized following literature procedures.[37,38]

$^1H$ and $^{31}P\{^1H\}$ NMR spectra were recorded with a Varian AS-400 spectrometer operating at 399.7 and 161.8 MHz, respectively. For $^1H$ NMR spectra, chemical shifts ($\delta$) were determined in parts per million (ppm) relative to the solvent residual peaks. For $^{31}P\{^1H\}$ NMR, chemical shifts were determined relative to concentrated $H_3PO_4$. Microanalyses (C, H, and N) were performed by Robertson Microlit Laboratories. Mass spectrometry was performed at the University of Cincinnati Mass Spectrometry facility. UV−vis spectra were collected on a Cary 500 spectrophotometer in HPLC grade solvents. Fluorescence measurements were carried out with a Cary Eclipse Spectrophotometer at room temperature. All samples were purged with argon for at least 15 min before the luminescence measurement.

**Synthesis.** *1,3-Bis(4-bromophenyl)-4-nitrobutan-1-one (Intermediate in the Synthesis of* $L_d$*).* (*E*)-1,3-bis(4-bromophenyl)prop-2-en-1-one (8.67 g, 23.7 mmol), nitromethane (7.22 g, 0.12 mol), and diethylamine (15.35 g, 0.21 mol) were combined in 250 mL of methanol and heated to reflux for 24 h. The resultant solution was evaporated to dryness, and solvents and volatile materials were removed. A brown oily solid was isolated. This material was used without further purification. Yield: 3.30 g, 33%. $^1H$ ($CDCl_3$) $\delta$ (ppm) 7.76−7.78 (m, 2H); 7.60−7.62 (m, 2H); 7.46−7.48 (m, 2H); 7.15−7.17 (m, 2H); 4.79 (dd, 1H, $J$ = 12.8 Hz, 6.8 Hz), 4.66 (dd, 1H, $J$ = 12.4 Hz, 8.0 Hz); 4.19 (quintet, 1H, $J$ = 6.8 Hz); 3.42 (d, 2H, $J$ = 6.8 Hz).

***L*$_d$.** 1,3-Bis(4-bromophenyl)-4-nitrobutan-1-one (3.30 g, 77.8 mmol) and ammonium acetate (30 g, 0.39 mol) were combined in 200 mL of 1-butanol and heated to reflux for 24 h. The solvent was stripped off and a dark residue was isolated. This residue was washed with hot methanol and vacuum filtration led to the isolation of a black solid. This material was used without further purification. Yield: 2.20 g, 74%. $^1H$ ($CDCl_3$) $\delta$ (ppm) 7.88 (d, 4H, $J$ = 8.8 Hz); 7.77 (d, 4H, $J$ = 8.4 Hz); 7.68 (d, 4H, $J$ = 8.4 Hz); 7.56(d, 4H, $J$ = 8.8 Hz); 7.52 (s, 2H).

***L*$_a$*Br*$_2$*-L*$_d$*Br*$_2$**.** **L** (1 equiv) was dissolved in 20 mL of dry $CH_2Cl_2$, and *N*-bromosuccinimide (2.2 equiv) was added. The solution was degassed under argon, and stirred vigorously under argon at room temperature. After several minutes, a precipitate was generated. The reaction mixture was kept under stirring overnight. Vacuum filtration led to the isolation of a black solid. This solid was washed several times with $CH_2Cl_2$, and dried under vacuum. Because of their limited solubility, $^1H$ NMR was only performed with $\mathbf{L_bBr_2}$. These compouds were directly used for the synthesis of gold(I) complexes. Yield: $\mathbf{L_aBr_2}$: 67%, $\mathbf{L_bBr_2}$: 77%, $\mathbf{L_cBr_2}$: 78%, $\mathbf{L_dBr_2}$: 79%. $^1H$ ($\mathbf{L_bBr_2}$, $CDCl_3$) $\delta$ (ppm) 8.04 (d, 4H, $J$ = 8.8 Hz); 7.77−7.82 (m, 4H); 7.35−7.49 (m, 6H); 7.05 (d, 4H, $J$ = 9.2 Hz), 3.91 (s, 6H).

***L*$_d$*AuPMe*$_2$*Ph (1).*** $\mathbf{L_d}$ (0.2186 g, 0.28 mmol) and NaO*t*Bu (0.0550 g, 0.57 mmol) were combined in 10 mL of dry THF. The mixture was purged with argon for 5 min and allowed to stir at room temperature under argon overnight. $Me_2PhPAuCl$ (0.1086 g, 0.29 mmol) was then transferred to the reaction mixture, and the resulting mixture was purged with argon for 5 min and allowed to stir at room temperature under argon for 48 h. THF was removed under vacuum, leaving a shiny residue. Benzene was added, and the solution was filtered through Celite. The filtrate was heated to 40 °C, and benzene was removed under vacuum. Trituration of the residue with pentane led to the isolation of a lustrous powder. This powder was then dissolved in benzene, and vapor diffusion of pentane into the benzene solution led to the isolation of dark red crystals. Yield: 0.1870 g, 58%. $^{31}P\{^1H\}$ ($C_6D_6$) $\delta$ (ppm): −1.61. $^1H$ ($C_6D_6$) $\delta$ (ppm): 8.10−8.13 (m, 4H), 7.78 (dd, 8H, $J$ = 8.4 Hz, 1.6 Hz), 7.42 (d, 4H, $J$ = 8.4 Hz), 7.23 (d, 4H, $J$ = 8.4 Hz), 7.12 (s, 2H), 6.80−7.00 (m, 5H), 0.53 (bs, 6H). Anal. Calcd. for $C_{40}H_{29}AuBr_4N_3P$: C, 43.71; H, 2.66; N, 3.82. Found: C, 43.83; H, 2.43; N, 3.63. UV−vis (2-MeTHF): $\lambda$ ($\varepsilon$) 316 nm ($6.16 \times 10^4$ $M^{-1}$ $cm^{-1}$), 610 nm ($5.36 \times 10^4$ $M^{-1}$ $cm^{-1}$); Emission (2-MeTHF, ex. 312 nm): 385 nm, 671 nm.

***L*$_a$*Br*$_2$*AuPMe*$_2$*Ph (2).*** $\mathbf{L_aBr_2}$ (0.0251 g, 0.04 mmol) and KO*t*Bu (0.0093 g, 0.08 mmol) were mixed in 10 mL of dry THF. The mixture was purged with argon for 5 min and allowed to stir at room temperature under argon overnight. $Me_2PhPAuCl$ (0.0130 g, 0.04 mmol) was then transferred to the reaction mixture. The resulting mixture was purged with argon for 5 min and allowed to stir at room temperature under argon for 48 h. THF was removed under vacuum, leaving a lustrous residue. Benzene was added, and the solution was filtered through Celite. The filtrate was heated to 40 °C, and benzene was removed under vacuum. Trituration of the residue with pentane led to the isolation of a lustrous powder. This powder was then dissolved in benzene, and vapor diffusion of pentane into the benzene solution led to the isolation of dark red crystals. Yield: 0.0210 g, 54%. $^{31}P\{^1H\}$ ($C_6D_6$) $\delta$ (ppm): −0.82. $^1H$ ($C_6D_6$) $\delta$ (ppm): 8.07−8.10 (m, 4H), 7.94−7.97 (m, 4H), 7.17−7.26 (m, 5H), 7.01−7.05 (m, 4H), 6.95−7.00 (m, 4H), 6.88−6.92 (m, 2H), 6.72−6.77 (m, 2H), 0.45 (d, 6H, $J$ = 10.4 Hz). Anal. Calcd. for $C_{40}H_{31}AuBr_2N_3P$: C, 51.03; H, 3.32; N, 4.46. Found: C, 51.30; H, 3.38; N, 4.20. UV−vis (2-MeTHF): $\lambda$ ($\varepsilon$) 309 nm ($3.40 \times 10^4$ $M^{-1}$ $cm^{-1}$), 585 nm ($8.45 \times 10^4$ $M^{-1}$ $cm^{-1}$); Emission (2-MeTHF, ex. 309 nm): 359 nm.

***L*$_b$*Br*$_2$*AuPMe*$_2$*Ph (3).*** $\mathbf{L_bBr_2}$ (0.1084 g, 0.16 mmol) and KO*t*Bu (0.0360 g, 0.32 mmol) were combined in 10 mL of dry THF. The mixture was purged with argon for 5 min and allowed to stir at room temperature under argon overnight. $Me_2PhPAuCl$ (0.0500 g, 0.16 mmol) was then transferred to the reaction mixture. The resulting mixture was purged with argon for 5 min and allowed to stir at room tempertaure (RT) under argon for 48 h. THF was removed under vacuum, leaving a lustrous residue. Benzene was added, and the solution was filtered through Celite. The filtrate was heated to 40 °C, and benzene was removed under vacuum. Trituration of the residue with pentane led to the isolation of a lustrous powder. This powder was then dissolved in benzene, and vapor diffusion of pentane into the benzene solution led to the isolation of dark red crystals. Yield: 0.0660 g, 39%. $^{31}P\{^1H\}$ ($C_6D_6$) $\delta$ (ppm): −0.85; $^1H$ ($C_6D_6$) $\delta$ (ppm): 8.11−8.13 (m, 4H), 8.00−8.02 (m, 4H), 7.25−7.29 (m, 5H), 6.89−6.99 (m, 3H), 6.78−6.86 (m, 2H), 6.65−6.67 (m, 5H), 3.21 (s, 6H), 0.54 (d, 6H, $J$ = 10.0 Hz). Anal. Calcd. for $C_{42}H_{35}AuBr_2N_3O_2P$: C, 50.37; H, 3.52; N, 4.20. Found: C, 50.10; H, 3.31; N, 4.18. HR-MS: Calcd. $m/z$ = 1002.05561 $(M+H)^+$, Found $m/z$ = 1002.05508. UV−vis (2-MeTHF): $\lambda$ ($\varepsilon$) 315 nm ($3.06 \times 10^4$ $M^{-1}$ $cm^{-1}$), 400 nm ($1.04 \times 10^4$ $M^{-1}$ $cm^{-1}$), 610 nm ($7.60 \times 10^4$ $M^{-1}$ $cm^{-1}$); Emission (2-MeTHF, ex. 315 nm): 372 nm, 467 nm, 670 nm.


dx.doi.org/10.1021/ic300709n | *Inorg. Chem.* 2012, 51, 7682−7688

***$L_cBr_2AuPMe_2Ph$ (4).*** $\mathbf{L_cBr_2}$ (0.0704 g, 0.11 mmol) and KO*t*Bu (0.0240 g, 0.22 mmol) were combined in 10 mL of dry THF. The mixture was purged with argon for 5 min and allowed to stir at room temperature under argon overnight. $Me_2PhPAuCl$ (0.0330 g, 0.11 mmol) was then transferred to the reaction mixture, and the resulting mixture was purged with argon for 5 min and allowed to stir at room temperature under argon for 48 h. THF was removed under vacuum, leaving a lustrous residue. Benzene was added, and the solution was filtered through Celite. The filtrate was heated to 40 °C, and benzene was removed under vacuum. Trituration of the residue with pentane led to the isolation of a lustrous powder. This powder was then dissolved in benzene, and vapor diffusion of pentane into the benzene solution led to the isolation of dark red crystals. Yield: 0.0300 g, 28%. $^{31}P\{^1H\}$ ($C_6D_6$) $\delta$ (ppm), −0.79; $^1H$ ($C_6D_6$) $\delta$ (ppm) 8.10−8.13 (m, 4H), 7.94−7.96 (m, 4H), 7.03−7.07 (m, 5H), 6.95−7.00 (m, 3H), 6.89−6.92 (m, 2H), 6.83−6.85 (m, 5H), 3.38 (s, 6 h), 0.49 (d, 6H, $J$ = 10.4 Hz). Anal. Calcd. for $C_{42}H_{35}AuBr_2N_3O_2P$: C, 50.37; H, 3.52; N, 4.20. Found: C, 50.65; H, 3.27; N, 4.01. UV−vis (2-MeTHF): $\lambda$ ($\varepsilon$) 312 nm ($8.6 \times 10^3$ $M^{-1}$ $cm^{-1}$), 595 nm ($5.47 \times 10^4$ $M^{-1}$ $cm^{-1}$); Emission (2-MeTHF, ex. 312 nm): 372 nm.

***$L_dBr_2AuPMe_2Ph$ (5).*** $\mathbf{L_dBr_2}$ (0.1040 g, 0.11 mmol) and KO*t*Bu (0.0240 g, 0.22 mmol) were combined in 10 mL of dry THF. The mixture was purged with argon for 5 min and allowed to stir at room temperature under argon overnight. $Me_2PhPAuCl$ (0.0330 g, 0.11 mmol) was then transferred to the reaction mixture. The resulting mixture was purged with argon for 5 min and allowed to stir at room temperature under argon for 48 h. THF was removed under vacuum, leaving a lustrous residue. Benzene was added, and the solution was filtered through Celite. The filtrate was heated to 40 °C, and benzene was removed under vacuum. Trituration of the residue with pentane led to the isolation of a lustrous powder. This powder was then dissolved in benzene, and vapor diffusion of pentane into the benzene solution led to the isolation of a dark greenish powder. Yield: 0.0638 g, 47%. $^{31}P\{^1H\}$ ($C_6D_6$) $\delta$ (ppm), −1.81; $^1H$ ($C_6D_6$) $\delta$ (ppm) 7.68−7.72 (m, 4H), 7.46−7.49 (m, 4H), 7.31−7.34 (m, 4H), 7.11−7.12 (m, 4H), 7.00−7.02 (m, 3H), 6.71−6.76 (m, 2H), 0.42 (d, 6H, $J$ = 10.4 Hz). Anal. Calcd. for $C_{40}H_{27}AuBr_6N_3P$: C, 38.22; H, 2.16; N, 3.34. Found: C, 38.15; H, 2.06; N, 3.14. UV−vis (2-MeTHF): $\lambda$ ($\varepsilon$) 315 nm ($3.54 \times 10^3$ $M^{-1}$ $cm^{-1}$), 605 nm ($7.24 \times 10^3$ $M^{-1}$ $cm^{-1}$); Emission (2-MeTHF, ex. 312 nm): 355 nm, 467 nm.

**X-ray Single Crystal Structure Analysis.** Single crystal X-ray data were collected on a Bruker AXS SMART APEX CCD diffractometer using monochromatic Mo K$\alpha$ radiation with the $\omega$ scan technique. The unit cells were determined using SMART[39] and SAINT+.[40] Data collection for all crystals was conducted at 100 K (−173.5 °C). All structures were solved by direct methods and refined by full matrix least-squares against $F^2$ with all reflections using SHELXTL.[41] Refinement of extinction coefficients was found to be insignificant. All non-hydrogen atoms were refined anisotropically. All hydrogen atoms were placed in standard calculated positions, and all hydrogen atoms were refined with an isotropic displacement parameter 1.2 times that of the adjacent carbon.

**Calculations.** Spin-restricted density-functional theory calculations were performed within Gaussian 09 rev. A.02.[42] Geometries were optimized without imposed symmetry. Calculations employed the exchange and correlation functionals of Perdew, Burke, and Ernzerhof,[43] and the TZVP basis set of Godbelt, Andzelm, and co-workers for carbon, hydrogen, oxygen, and phosphorus.[44] For gold, the Stuttgart 97 effective core potential and basis set were used;[45] scalar relativistic effects are included implicitly. Harmonic frequency calculations returned all real vibrational frequencies. The calculations, including geometry optimizations, impose continuum solvation in THF, using the integral equation formalism of Tomasi's polarizable continuum model.[46−49] Population analyses were performed with the AOMIX-CDA software of Gorelsky.[50,51]

## ■ ASSOCIATED CONTENT

### Ⓢ Supporting Information

Absorption and emission of **2**, **3**, and **4**; Kohn−Sham orbital energy level diagrams of **2**−**5**, and optimized Cartesian coordinates of **1**−**5** calculated by density-functional theory as described in the Experimental Section. This material is available free of charge via the Internet at http://pubs.acs.org.

## ■ AUTHOR INFORMATION

### Corresponding Author

*E-mail: tgray@case.edu.

### Notes

The authors declare no competing financial interest.

## ■ ACKNOWLEDGMENTS

The authors thank the National Science Foundation (Grant CHE-1057659 to T.G.G.) for support. The diffractometer at Case Western Reserve was funded by NSF Grant CHE-0541766. N.D. thanks the Republic of Turkey for a fellowship. We thank Dr. T. S. Teets for experimental assistance and Professor D. G. Nocera (both then at the Massachusetts Institute of Technology) for access to instrumentation. We thank also Dr. Matthias Zeller, Youngstown State University, for assistance with the crystallography.

## ■ REFERENCES

(1) Gorman, A.; Killoran, J.; O'Shea, C.; Kenna, T.; Gallagher, W. M.; O'Shea, D. F. *J. Am. Chem. Soc.* **2004**, *126*, 10619−10631.
(2) Killoran, J.; Allen, L.; Gallagher, J. F.; Gallagher, W. M.; O'Shea, D. F. *Chem. Commun.* **2002**, 1862−1863.
(3) Gao, L.; Senevirathna, W.; Sauvé, G. *Org. Lett.* **2011**, *13*, 5354−5357.
(4) Coskun, A.; Yilmaz, M. D.; Akkaya, E. U. *Org. Lett.* **2007**, *9*, 607−609.
(5) Loudet, A.; Bandichhor, R.; Burgess, K.; Palma, A.; McDonnell, S. O.; Hall, M. J.; O'Shea, D. F. *Org. Lett.* **2008**, *10*, 4771−4774.
(6) Teets, T. S.; Partyka, D. V.; Updegraff, J. B., III; Gray, T. G. *Inorg. Chem.* **2008**, *47*, 2338−2346.
(7) Partyka, D. V.; Deligonul, N.; Washington, M. P.; Gray, T. G. *Organometallics* **2009**, *28*, 5837−5840.
(8) Teets, T. S.; Partyka, D. V.; Esswein, A. J.; Updegraff, J. B., III; Zeller, M.; Hunter, A. D.; Gray, T. G. *Inorg. Chem.* **2007**, *46*, 6218−6220.
(9) Teets, T. S.; Updegraff, J. B., III; Esswein, A. J.; Gray, T. G. *Inorg. Chem.* **2009**, *48*, 8134−8144.
(10) Palma, A.; Gallagher, J. F.; Müller-Bunz, H.; Wolowska, J.; McInnes, E. J. L.; O'Shea, D. F. *Dalton Trans.* **2009**, 273−279.
(11) Gouterman, M. In *The Porphyrins*; Dolphin, D., Ed.; Academic: New York, 1978; pp 1−165.
(12) Qian, G.; Wang, Z. Y. *Chem.—Asian J.* **2010**, *5*, 1006−1029.
(13) Escobedo, J. O.; Rusin, O.; Lim, S.; Strongin, R. M. *Curr. Opin. Chem. Biol.* **2010**, *14*, 64−70.
(14) Partyka, D. V.; Zeller, M.; Hunter, A. D.; Gray, T. G. *Angew. Chem., Int. Ed.* **2006**, *45*, 8188−8191.
(15) Partyka, D. V.; Esswein, A. J.; Zeller, M.; Hunter, A. D.; Gray, T. G. *Organometallics* **2007**, *26*, 3279−3282.
(16) Gao, L.; Peay, M. A.; Partyka, D. V.; Updegraff, J. B., III; Teets, T. S.; Esswein, A. J.; Zeller, M.; Hunter, A. D.; Gray, T. G. *Organometallics* **2009**, *28*, 5669−5681.
(17) Vogt, R. A.; Peay, M. A.; Gray, T. G.; Crespo-Hernández, C. E. *J. Phys. Chem. Lett.* **2010**, *1*, 1205−1211.
(18) Gao, L.; Partyka, D. V.; Updegraff, J. B., III; Deligonul, N.; Gray, T. G. *Eur. J. Inorg. Chem.* **2009**, 2711−2719.
(19) Partyka, D. V.; Gao, L.; Teets, T. S.; Updegraff, J. B., III; Deligonul, N.; Gray, T. G. *Organometallics* **2009**, *28*, 6171−6182.

(20) Partyka, D. V.; Teets, T. S.; Zeller, M.; Updegraff, J. B., III; Hunter, A. D.; Gray, T. G. *Chem.—Eur. J.* **2012**, *18*, 2100−2112.
(21) Gao, L.; Niedzwiecki, D. S.; Deligonul, N.; Zeller, M.; Hunter, A. D.; Gray, T. G. *Chem.—Eur. J.* **2012**, *18*, 6316−6327.
(22) Chao, H.-Y.; Lu, W.; Li, Y. Q.; Chan, M. C. W.; Che, C.-M.; Cheung, K.-K.; Zhu, N. *J. Am. Chem. Soc.* **2002**, *124*, 14696−14706.
(23) Meyer, N.; Lehmann, C. W.; Lee, T. K.-M.; Rust, J.; Yam, V. W.-W.; Mohr, F. *Organometallics* **2009**, *28*, 2931−2934.
(24) Heng, W. Y.; Hu, J.; Yip, J. H. K. *Organometallics* **2007**, *26*, 6760−6768.
(25) Ulrich, G.; Ziessel, R.; Haefele, A. *J. Org. Chem.* **2012**, *77*, 4298−4311.
(26) Tolman, C. A. *Chem. Rev.* **1977**, *77*, 313−348.
(27) Stout, G. H.; Jensen, L. H. *X-Ray Structure Determination: A Practical Guide*; Wiley-Interscience: New York, 1989, pp 404−405.
(28) Gray, T. G. *Comments Inorg. Chem.* **2007**, *28*, 181−212.
(29) Abdou, H. E.; Mohamed, A. A.; Fackler, J. P., Jr. In *Gold Chemistry: Applications and Future Directions in the Life Sciences*; Mohr, F., Ed.; Wiley-VCH: Weinheim, Germany, 2009, pp 1−45.
(30) Coco, S.; Espinet, P. In *Gold Chemistry: Applications and Future Directions in the Life Sciences*; Mohr, F., Ed.; Wiley-VCH: Weinheim, Germany, 2009, pp 357−396.
(31) Schmidbaur, H.; Grohmann, A.; Olmos, M. E. Organogold Chemistry. In *Gold: Progress in Chemistry, Biochemistry and Technology*; Schmidbaur, H., Ed.; Wiley: Chichester, U.K., 1999.
(32) Schmidbaur, H.; Schier, A. In *Comprehensive Organometallic Chemistry III*; Crabtree, R. H., Mingos, D. M. P., Eds.; Elsevier: Amsterdam, The Netherlands, 2006; Vol. *2*, Section 2.05.
(33) Clegg, W. *Acta Crystallogr.* **1976**, *B32*, 2712−2714 ; Estimated standard deviations for this structure are stated to be 0.001−0.003 Å in distances involving Au or P, and 0.1° for angles involving these atoms.
(34) Meiners, J.; Herrmann, J.-S.; Roesky, P. W. *Inorg. Chem.* **2007**, *46*, 4599−4604.
(35) Mulliken, R. S. *J. Chem. Phys.* **1955**, *23*, 1833−1840.
(36) Rachford, A. A.; Ziessel, R.; Bura, T.; Retailleau, P.; Castellano, F. N. *Inorg. Chem.* **2010**, *49*, 3730−3736.
(37) Mann, F. G.; Wells, A. F.; Purdie, D. *J. Chem. Soc.* **1937**, 1828−1936.
(38) Schneider, D.; Schier, A.; Schmidbaur, H. *Dalton Trans.* **2004**, 1995−2005.
(39) *SMART for WNT/2000*, Version 5.628; Bruker AXS Inc.: Madison, WI, 1997−2002.
(40) *SAINT*, Version 6.45; Bruker AXS Inc.: Madison, WI, 1997−2003.
(41) *SHELXTL*, Version 6.10; Bruker AXS Inc.: Madison, WI, 2000.
(42) Frisch, M. J.; Trucks, G. W.; Schlegel, H. B.; Scuseria, G. E.; Robb, M. A.; Cheeseman, J. R.; Scalmani, G.; Barone, V.; Mennucci, B.; Petersson, G. A.; Nakatsuji, H.; Caricato, M.; Li, X.; Hratchian, H. P.; Izmaylov, A. F.; Bloino, J.; Zheng, G.; Sonnenberg, J. L.; Hada, M.; Ehara, M.; Toyota, K.; Fukuda, R.; Hasegawa, J.; Ishida, M.; Nakajima, T.; Honda, Y.; Kitao, O.; Nakai, H.; Vreven, T.; Montgomery, J. A.; , Jr., Peralta, J. E.; Ogliaro, F.; Bearpark, M.; Heyd, J. J.; Brothers, E.; Kudin, K. N.; Staroverov, V. N.; Kobayashi, R.; Normand, J.; Raghavachari, K.; Rendell, A.; Burant, J. C.; Iyengar, S. S.; Tomasi, J.; Cossi, M.; Rega, N.; Millam, J. M.; Klene, M.; Knox, J. E.; Cross, J. B.; Bakken, V.; Adamo, C.; Jaramillo, J.; Gomperts, R.; Stratmann, R. E.; Yazyev, O.; Austin, A. J.; Cammi, R.; Pomelli, C.; Ochterski, J. W.; Martin, R. L.; Morokuma, K.; Zakrzewski, V. G.; Voth, G. A.; Salvador, P.; Dannenberg, J. J.; Dapprich, S.; Daniels, A. D.; Ö. Farkas, Foresman, J. B.; Ortiz, J. V.; Cioslowski, J.; , Fox, D. J. *Gaussian 09*, Revision A.02; Gaussian, Inc.: Wallingford, CT, 2009.
(43) Perdew, J. P.; Burke, K.; Ernzerhof, M. *Phys. Rev. Lett.* **1996**, *77*, 3865−3868.
(44) Godbout, N.; Salahub, D. R.; Andzelm, J.; Wimmer, E. *Can. J. Chem.* **1992**, *70*, 560−571.
(45) Dolg, M.; Wedig, U.; Stoll, H.; Preuss, H. *J. Chem. Phys.* **1987**, *86*, 866−872.
(46) Miertus, S.; Scrocco, E.; Tomasi, J. *Chem. Phys.* **1981**, *55*, 117−129.
(47) Tomasi, J.; Mennucci, B.; Cammi, R. *Chem. Rev.* **2005**, *105*, 2999−3093.
(48) Cancès, E.; Mennucci, B.; Tomasi, J. *J. Chem. Phys.* **1997**, *107*, 3032−3041.
(49) Mennucci, B.; Cancès, E.; Tomasi, J. *J. Phys. Chem. B* **1997**, *101*, 10506−10517.
(50) Gorelsky, S. I. *AOMix: Program for Molecular Orbital Analysis*, version 6.5; University of Ottawa: Ottawa, Canada, 2011; http://www.sg-chem.net.
(51) Gorelsky, S. I.; Lever, A. B. P. *J. Organomet. Chem.* **2001**, *635*, 187−196.